Supporting Information For:

A novel poly(polyoxometalate) built by $\{Cu_9\}/\{Cu_5\}$ clusters and $\{PW_9\}/\{PW_{10}\}/\{PW_{11}\}$ lacunary fragments

Wei-Hui Fang,[a] Wei-Dong Wang,[a] and Guo-Yu Yang*[a,b]

[a] *State Key Laboratory of Structural Chemistry, Fujian Institute of Research on the Structure of Matter, Chinese Academy of Sciences, Fuzhou, Fujian 350002, China. E-mail: ygy@fjirsm.ac.cn*
[b] *Department of Chemistry, Beijing Institute of Technology, Beijing 100081, China. E-mail: ygy@bit.edu.cn*

Content

Experimental Section:

Materials and physical measurements: $Na_9[A\text{-}\alpha\text{-}PW_9O_{34}]\cdot 7H_2O$ is synthesized according to the literature.[1] The other chemicals were commercially purchased and used without further purification. The elemental analyses for C, H, N were performed on a Vario EL **III** elemental analyzer. The FT-IR spectra (KBr pellets) were recorded by using an ABB Bomen MB 102 spectrometer over a range 400-4000 cm^{-1}. Thermogravimetric analyses were performed on a Mettler TGA/SDTA 851^e analyzer with a heating rate of 10 °C/min from 30 to 1000 °C under air atmosphere. Powder X-ray diffraction (PXRD) data were collected on a Rigaku Mini Flex **II** diffractometer using Cu K_α radiation (λ=1.54056Å) under ambient conditions. ICP analyses of P, Cu and W were conducted on an Ultima2 spectrometer. The UV diffuse reflection data were recorded at room temperature using a powder sample with $BaSO_4$ as a standard (100% reflectance) on a PerkinElmer Lamda-950 UV spectrophotometer and scanned at 200-800 nm. The band gap (Eg) was determined as the intersection point between the energy axis and the line extrapolated from the linear portion of the absorption edge in a plot of Kubelka-Munk function against energy E. Kubelka-Munk function,[2] α/S = (1–R)2/2R, was converted from the recorded diffuse reflectance data, where α is the absorption coefficient, S is the scattering coefficient, R is the reflectance of an infinitely thick layer at a given wavelength. Magnetic measurements were performed on a MPMS XL magnetometer in the temperature range from 2 to 300 K at an applied magnetic field of 2 kOe.

Synthesis of $[\{Cu_6(\mu_3\text{-}OH)_3(en)_3(H_2O)_3\}(B\text{-}\alpha\text{-}PW_9O_{34})]\cdot 7H_2O$

$Na_9[A\text{-}\alpha\text{-}PW_9O_{34}]\cdot 7H_2O$ (PW_9)[1] (0.256 g, 0.1 mmol), $CuCl_2\cdot 2\,H_2O$ (0.170 g, 1.0 mmol), en (0.05 mL, 0.75 mmol), and acetate (0.10 mL, 1.75 mmol) were successively added into distilled water (5 mL, 278 mmol). Being stirred at room temperature for 30 min (pH 3.9), the mixture was sealed in a 30 mL Teflon-lined stainless steel autoclave, heated under autogeneous pressure at 80 ºC for 5 days, and then cooled to room temperature naturally in air (pH 3.8). Green strips of crystals were collected by filtration, washed with distilled water, and dried in air. Yield: 13% (based on PW_9).

X-ray crystallography: A suitable single crystal of compound **1** was mounted on a glass fiber for indexing and intensity data were collected at 293 K on Rigaku SATURN70 CCD diffractometer with a graphite-monochromatized Mo Kα (λ=0.71073 Å). All absorption corrections were performed by using the SADABS program. Direct methods were used to solve the structures and to locate the heavy atoms using the SHELXTL-97 program package.[3] The remaining atoms were found from successive full-matrix least-squares refinements on F^2. All non-H atoms were refined anisotropically except for free water molecules and some carbon atoms.The Cu9 and W31 atoms were disordered with the occupation factors of 0.75 and 0.25, respectively. Residual electron density located in these voids was unable to be assigned unambiguously and so was treated with SQUEEZE. CCDC-807965 contain the supplementary crystallographic data for this paper for compound **1**. These data can be obtained free of charge from the Cambridge Crystallographic Data Centre via www.ccdc. cam.ac.uk/ data_request/ cif.

1 A. P. Ginsberg, Wiley, New York, 1990, vol. 27, p. 100.

2 W. M. Wesley, W. G. H. Harry, *Reflectance Spectroscopy*; Wiley: New York, 1966, pp104-169.

3 (a) G. M. Sheldrick, *SHELXL97, Program for Crystal Structure Refinement (University of Göttingen, Göttingen, Germany, 1997)*; (b) G. M. Sheldrick, *SHELXS97, Program for Crystal Structure Solution (University of Göttingen, Göttingen, Germany, 1997).*

Supporting Figures and Table:

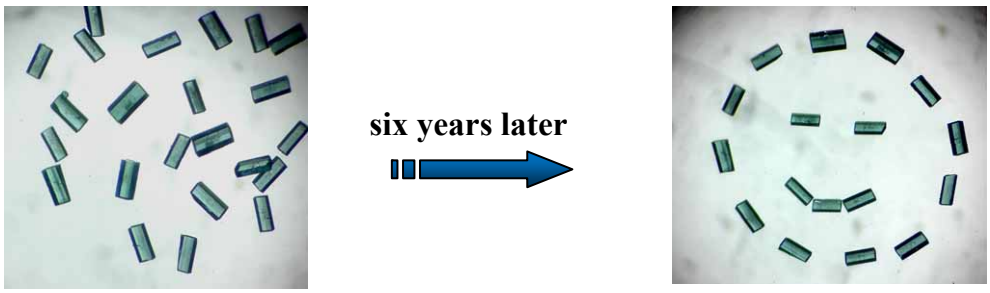

Fig. S1. The photographs of the crystalline sample in 2009 and at present.

Table S1 The comparison of cell parameters of the crystalline sample in 2009 and at present

	2009	at present
Crystal system	Triclinic	Triclinic
Space group	$P\bar{1}$	$P\bar{1}$
a/Å	12.159(3)	12.140(1)
b/Å	22.224(4)	22.187(2)
c/Å	30.636(6)	30.578(3)
α/°	92.391(3)	92.328(1)
β/°	97.373(3)	97.434(1)
γ/°	95.874(3)	95.995(1)
V/Å^3	8154(3)	8110.7(1)
Temperature/K	293(2)	293(2)

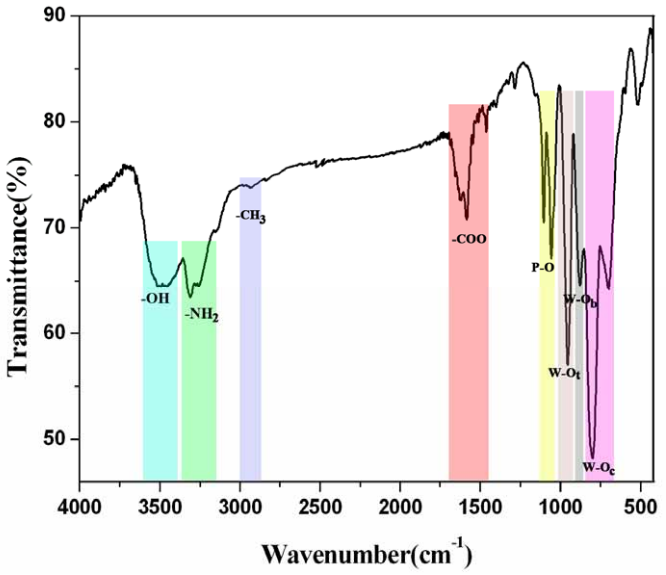

Fig. S2. IR spectrum of compound **1**.

As shown in Fig. S2, the big absorb band from 4000-1500 cm^{-1} generally attribute to the organic functional groups, and the characteristic vibrations in the region 1100-700 cm^{-1} are derived from the inorganic Keggin POTs. The stretching bands of the -OH, –NH_2, and –CH_3 groups are observed at 3550-3400, 3350-3150, and 2980-2930 cm^{-1}, respectively. The vibrations at about 1600 to 1400 cm^{-1} are corresponding to the asymmetric and stretching vibrations of the carboxyl group, respectively. In addition, the bands at around 1110 and 1050 cm^{-1} can be assigned to the ν(P-O) stretching vibration. The ν(W-O) stretching vibration bands resulting from the Keggin-type POT framework, namely, ν(W-O_t), ν(W-O_b) and ν(W-Oc) appear at 954, 880, 800-695 cm^{-1}, respectively.

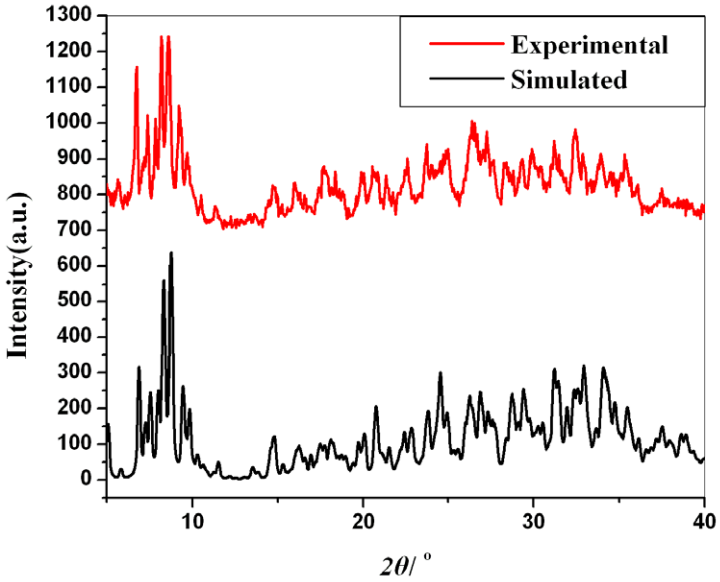

Fig. S3. The experimental PXRD pattern of compound **1** and the simulated PXRD pattern derived from the single crystal X-ray diffraction data.

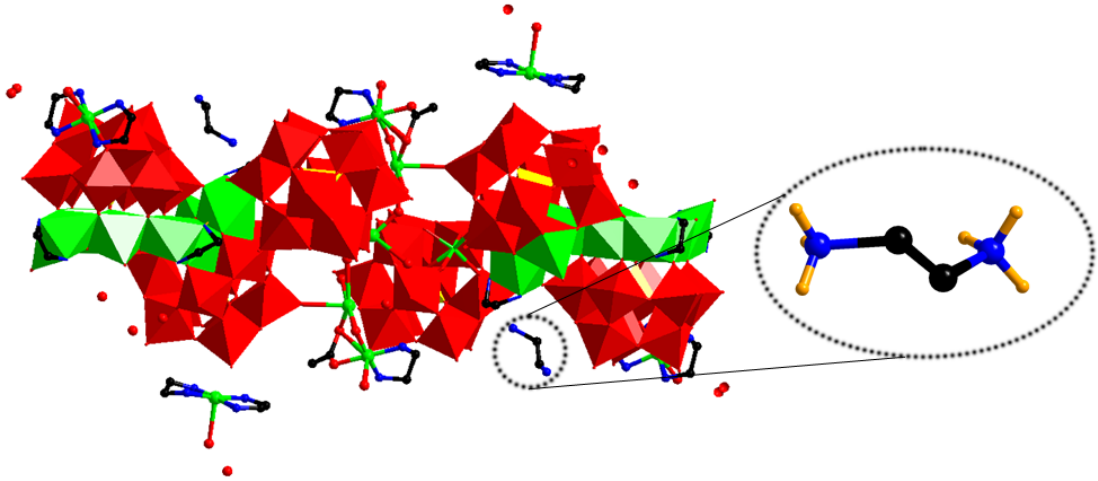

Fig. S4. The molecular structure of compound **1** and the zoom view of the doubly protonated en. Color code: WO_6 red, PO_4 yellow, CuO_xN_y green, Cu green, C black, N blue, O red, H yellow.

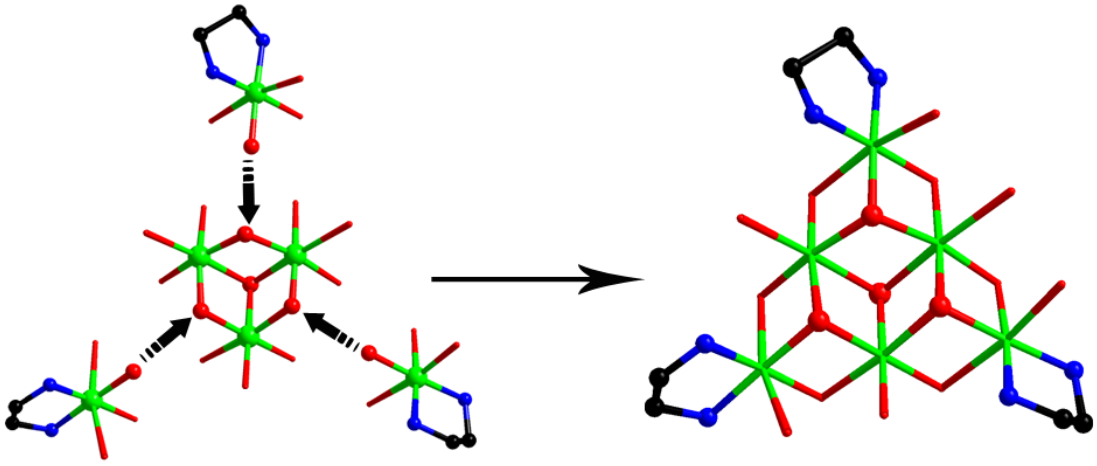

Fig. S5. The scheme representation of the assembly of the $\{Cu_6\}$ cluster. The μ_3-OH bridges are emphasised in ball view.

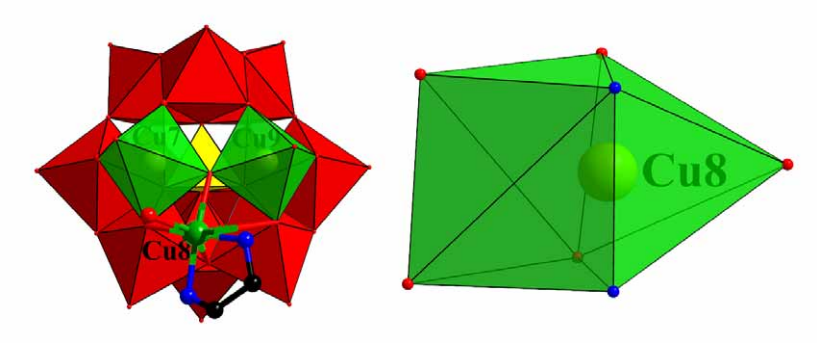

Fig. S6. Polyhedral view of $\{Cu_3PW_{10}\}$ and coordination environment of Cu8.

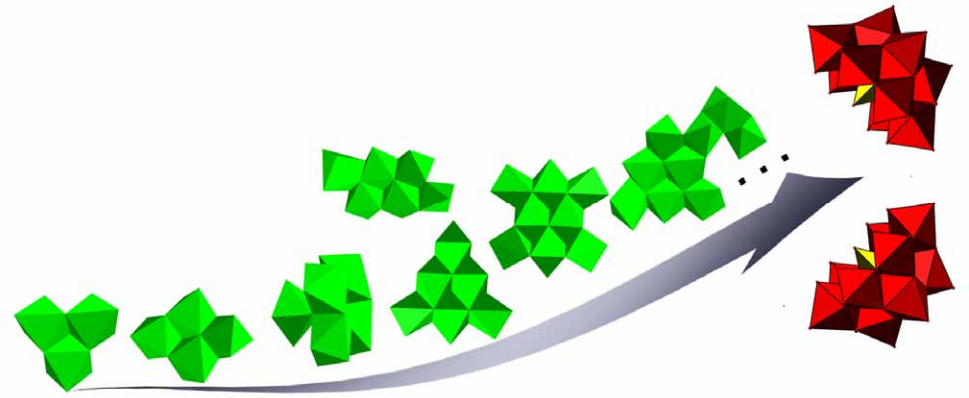

Fig. S7. Schematic illustration of the assembly of the sandwich Cu-substituted dimer. Red polyhedra WO_6, yellow polyhedra PO_4, green polyhedra CuO_xN_y.

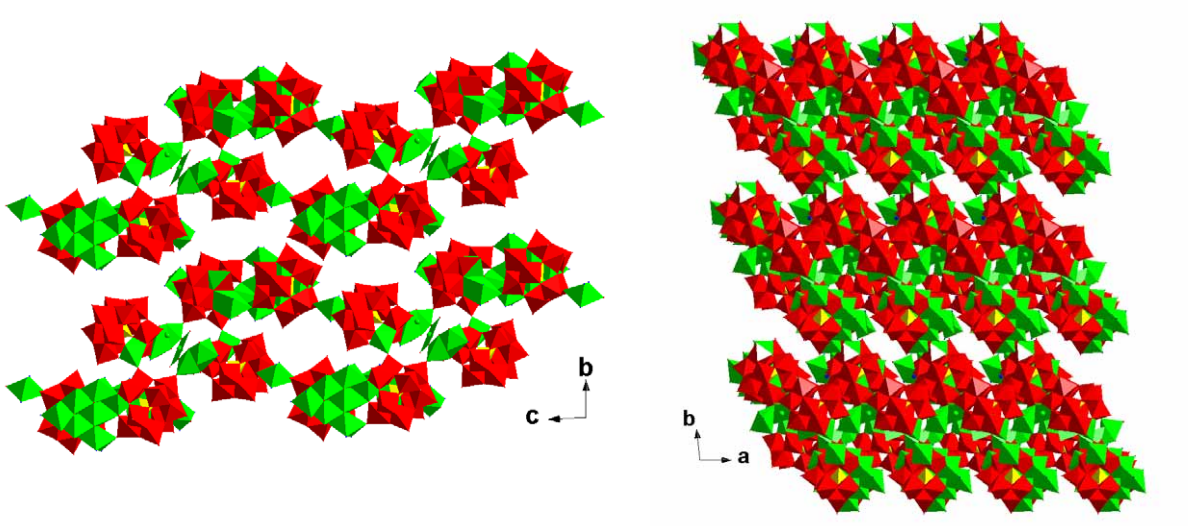

Fig. S8. View of the hexamers on bc plan (left) and stacking mode along the c-axis (right). Red polyhedra WO_6, yellow polyhedra PO_4, green polyhedra CuO_xN_y.

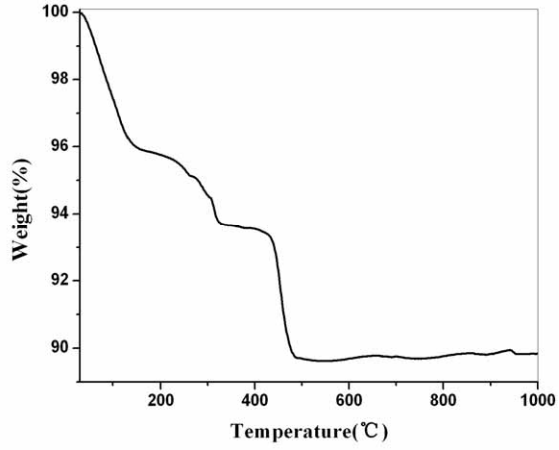

Fig. S9. TG curve of compound **1**.

As shown Fig. S9, the TG thermal behaviour of compound **1** was investigated on crystalline samples under an air atmosphere from 30 to 1000 °C. The TG curve indicates compound **1** undergo three steps of weight loss. The first step weight loss from 30-135°C (3.88%) corresponds to the release of water molecules and acetate (calcd. 3.78%). The following weight loss from 135-325°C is 2.36% (calcd. 2.31%), involving the removal of hydroxyl groups and seven en ligands. The third weight loss of 4.07% from 325-500°C approximately assigned to the decomposition of the left twelve en ligands (calcd. 3.85%). Assuming that the residue corresponds to CuO, P_2O_5 and WO_3, the observed weight (89.69%) is in good agreement with the calculated value (90.06%).

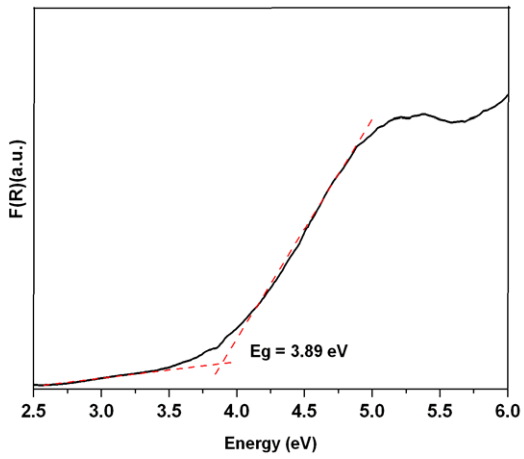

Fig. S10. Plots of Kunelka-Munk function versus energy Eg (eV) for compound **1**.

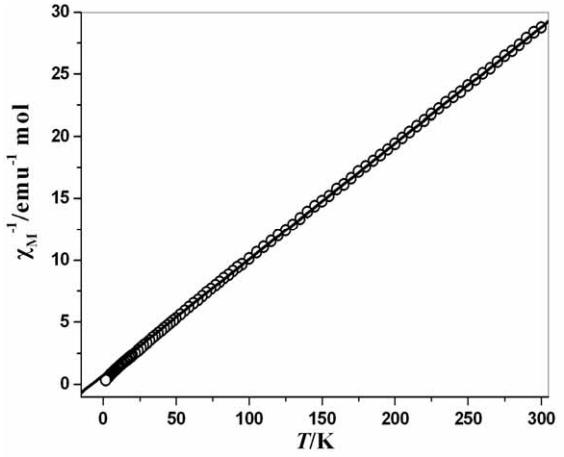

Fig. S11. Temperature dependence of χ_M^{-1} for **1**. The solid line is the best-fit according to the Curie-Weiss law.